

# A Novel Framework for Accurate Brain Tumor Detection in MRI Scans Using CNN, MLP, and KNN Techniques

Mohammad Anwar Assaad<sup>1,\*</sup>

<sup>1</sup>Department of Informatics and Software Engineering, College of Engineering,  
Cihan University-Erbil, Kurdistan Region, Iraq  
mohammad.anwar@cihanuniversity.edu.iq

Maral Ismael Saleh<sup>2</sup>

<sup>2</sup>College of Science, Kirkuk University, Kirkuk, Iraq  
maralismail92@gmail.com

Rania Mahrousseh<sup>3</sup>

<sup>3</sup>Al-Sham Private University, Latakia Colleges, Syria  
mahroussehrania@gmail.com

\*Corresponding author: Mohammad Anwar Assaad

Received January 20, 2025, revised March 18, 2025, accepted March 20, 2025.

---

**ABSTRACT.** *Brain tumors are among the most sensitive tumors that must be detected in their very early stages, otherwise they will lead to irreparable problems in the body later, because the brain is responsible for all commands and functions in the human body. Brain tumors occur as a result of the rapid, random and uncontrolled growth of brain cells, and if not treated in the early stages, they can lead to major problems and even death. The main challenge in detecting brain tumors lies in the differences in the location, shape and size of the tumor, also the tumor in its early stages is too small to be noticed by the human eye in MRI images, thus doctors may misdiagnose the disease in its early stages. In response to these challenges, this research focuses on developing an approach to detect brain tumors in MRI images using a combination of deep learning and machine learning techniques. Convolutional neural networks (CNNs) will be used to extract key features from MRI images and capture complex spatial patterns, after that, the extracted features are then processed by a multi-layer perceptron (MLP) network to reduce the features space. The MLP network undergoes a novel training process where each batch is divided into training and test sets of equal size from each class and then the reference point is calculated based on the arithmetic mean of each feature, after that, the Euclidean distance is used to classify the test samples followed by the backpropagation error process to adjust the network weights. After optimizing the feature space, the K-nearest neighbors (KNN) algorithm is used for the final classification where KNN training involves dividing the batches into training and test sets and extracting the performance metrics across all epochs. The proposed model achieved an accuracy of 97% compared to the custom CNN algorithm which achieved an accuracy of 90%.*

**Keywords:** Convolution Neural Network, CNN, Multi-layers Perceptron, MLP, K-nearest Neighbors, KNN, Brain Tumor, Deep Learning, Machine Learning

---

**1. Introduction.** Brain tumors are among the most common types of tumors that directly affect the central nervous system, which may lead to various disabilities that can occur and often lead to death. Accurate and early diagnosis of the tumor in its early stages is of great importance in order to carry out appropriate therapeutic interventions in a timely manner, which in turn leads to reducing the mortality rates resulting from brain tumors [1]. Magnetic resonance imaging (MRI) is one of the most widely used medical imaging methods in detecting tumors in general due to its high accuracy and ability to show and display detailed anatomical structures of the area to be imaged in the human body [2]. Despite the effectiveness and accuracy of MRI images, they require interpretation by doctors specialized in radiology images. Therefore, this manual interpretation is often subject to human error, especially in distinguishing between different types of tumors and detecting tumors in their early stages, as it is difficult to notice the presence of a tumor in the image due to its small size in its early stages [3]. As a result of these challenges, there has been an urgent need to develop systems capable of automated detection of brain tumors, as these systems benefit from artificial intelligence techniques, both machine learning and deep learning, to support medical decision-making for radiologists and improve diagnostic accuracy. Convolutional neural networks (CNNs) have emerged, which have achieved exceptional results in the field of pattern recognition in images, thanks to their great ability to extract subtle and deep features hidden within image pixels. This has made this type of network ideal for use in the process of extracting features from images in general and MRI images in particular, as this is considered a very important step to distinguish between healthy and infected tissues, as well as to determine the type and stage of the tumor [4,5]. Despite the great benefits of CNNs and their ability to extract features accurately, they suffer from the high-dimensional feature space they generate, which may lead to computational inefficiency, noise, or repetition that can affect the performance of the algorithm [6]. In order to solve the problem of the high-dimensional feature space resulting from CNNs, we propose in this paper a hybrid approach that integrates a multi-layer Perceptron (MLP) network to reduce the space of features extracted using CNNs [7]. In this paper, the MLP network will be trained in a new batch method that ensures balanced learning across all classes by calculating a reference point for each class in the dataset by calculating the arithmetic mean of all samples for each class, producing a single sample for each class containing the arithmetic mean value for each feature, where this sample represents the reference point for the class and is represented within a multidimensional space. This process improves the feature space, making it easier to distinguish between tumor types and more computationally efficient to run the model in low-resource environments. The proposed feature space reduction method takes advantage of the back-propagation error to adjust the network weights and optimize the new feature values, resulting in a dynamic feature reduction method that is adaptive across diverse datasets and is able to make distinguishing between tumor types easier and more computationally efficient, which enables the model to run in low-resource environments. For the final classification process, the K-Nearest Neighbors (KNN) algorithm is used.

Following previous works [8–15], the proposed hybrid approach helps to increase the model's adaptability to different data types, reduce overfitting, enhance the model generalization capabilities and thus maintain the model's sustainability. The proposed approach helps to address the major challenges of high-dimensional feature spaces and overfitting issues. The proposed model helps radiologists in supporting decision making and making accurate and timely diagnoses and paves the way for the development of advanced AI-based tools in healthcare applications.

**2. Literature review.** The study [16] presents a methodology for classifying brain tumors in MRI images based on a pre-trained model, ResNet-101. The study relied on a dataset that includes three different types of brain tumors (glioma, pituitary tumor, and meningioma). The study used zero-centered density normalization and data augmentation techniques for improving the accuracy. The results achieved significant improvements in accuracy, specificity, and sensitivity compared to other state-of-the-art methods.

The study [17] explored the ability of pre-trained deep convolutional neural models, such as VGG-19, VGG-16, ResNet-50, and Inception V3, to classify MRI brain tumor images. It used data augmentation and transfer learning to improve the performance of the models.

The study [18] used 64 fully connected neurons with two convolutional layers to classify brain tumor in MRI images. The study didn't use all the available data in dataset, instead of this, the researchers used 700 images for each class to balance the samples of each class. The achieved classification accuracy was 84.1%.

The study [19] presented a classification model based on CNN consisting of four convolutional layers in addition to a set of normalization layers, three max pooling layers, and a final fully connected layer. 70% of the data was used for training and 30% for testing using 10-fold cross-validation. The model achieved a classification accuracy of 81.0%.

The study [20] relied on segmenting brain tumor regions in MRI images using augmented region growth approach using BraTS2015 dataset. The proposed approach in this study is based on image processing using a thresholding approach where the image is divided into eight blocks to estimate the intensity of each region. Then, a region growth algorithm is applied to accurately identify the tumor region and then deep learning is used to identify the tumor. The proposed model achieved a classification accuracy of 90%.

**3. Methodology.** The proposed methodology includes building and training a CNN network to extract deep features from brain MRI images. Then, a Multilayers Perceptron artificial neural network is used for the feature reduction process and then the KNN algorithm is used for the classification process. These steps will be implemented using the KERAS framework in the PYTHON programming language [21]. Figure 1 illustrates the overall framework of the proposed methodology.

**3.1. Data collection.** The dataset used includes 5712 MRI images, each image has a size 512 x 512. All images are grayscale MRI scans that highlight different brain structures, making them suitable for tumor detection tasks. The dataset includes two folders, the first folder for training and the second folder for testing. Each folder contains four folders, each of them represents one class which is ('glioma', 'meningioma', 'no-tumor', 'pituitary'). The dataset is obtained from Kaggle [22].

**3.2. Data processing.** This phase encompasses a series of image processing techniques applied to the dataset's images. Enhancing the image data and boosting the diversity of the training dataset can be performed by using these operations and applying various transformations to the images [23]. A pixel normalization process is also performed to standardize the input data and facilitate efficient model training. The objective is to enhance the model's ability to generalize to new data [24, 25]. Below we explain the preprocessing operations that are applied to the images:

- **rescale=1./255:** This parameter normalizes pixel values to a range of 0 to 1 by dividing each value by 255, facilitating faster convergence of the neural network.
- **rotation\_range=40:** Randomly rotates the image by a specified angle, up to a maximum of 40 degrees in this case.

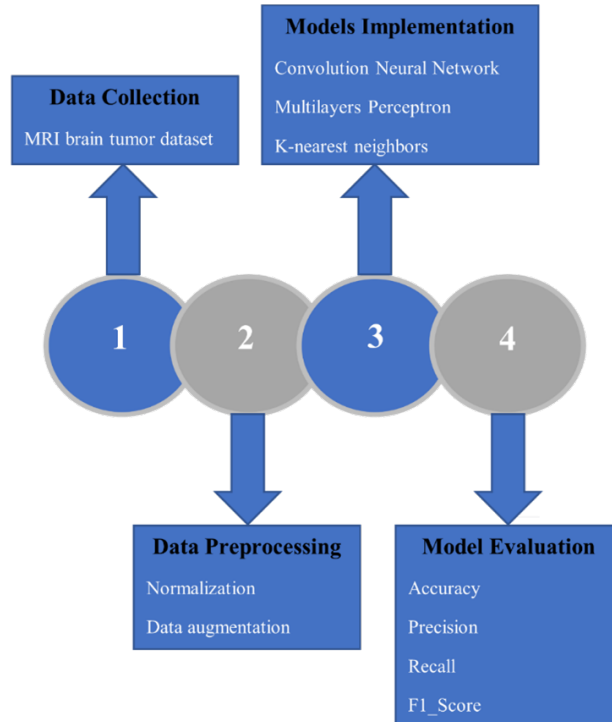


FIGURE 1. The overall framework of the proposed methodology

- `width_shift_range=0.2` and `height_shift_range=0.2`: Randomly adjusts the width and height of the image by a small fraction of their total dimensions, up to 20% in this case.
- `shear_range=0.2`: Applies a shear transformation with a maximum intensity of 20%.
- `zoom_range=0.2`: Randomly zooms into the image by a factor of up to 20%.
- `horizontal_flip=True`: Randomly performs horizontal flips on the images.
- `fill_mode='nearest'`: This parameter specifies the strategy for filling new pixels introduced during rotation or transformation. Using "nearest" assigns the value of the closest pixel to fill the empty areas.

**3.3. Models Implementations.** First, the CNN model shown in Figure 2 will be built. The model will be trained, performance metrics will be extracted, then the features of the penultimate dense layer will be used and fed into the MLP model to reduce the features, then KNN will be used to extract the performance metrics and compare them with the basic CNN model.

As mentioned earlier, the feature reduction process is done using a Multilayers Perceptron type artificial neural network [26]. The proposed artificial neural network consists of an input layer followed by a hidden layer containing 18 artificial neurons followed by a second hidden layer consisting of 10 artificial neurons and then an output layer consisting of 5 artificial neurons. The MLP network undergoes a new training process where each batch is divided into training and test sets of equal size from each class. The reference points for each class are calculated based on the arithmetic mean of each feature, and the Euclidean distance is used to classify the test samples, followed by a back-propagation error process to adjust the network weights. The goal of this network is to reduce the feature space from 128 (the number of features extracted using CNN) to 5 features. Figure 3 shows the proposed neural network structure. Figure 4 illustrates the training mechanism of the proposed artificial neural network.

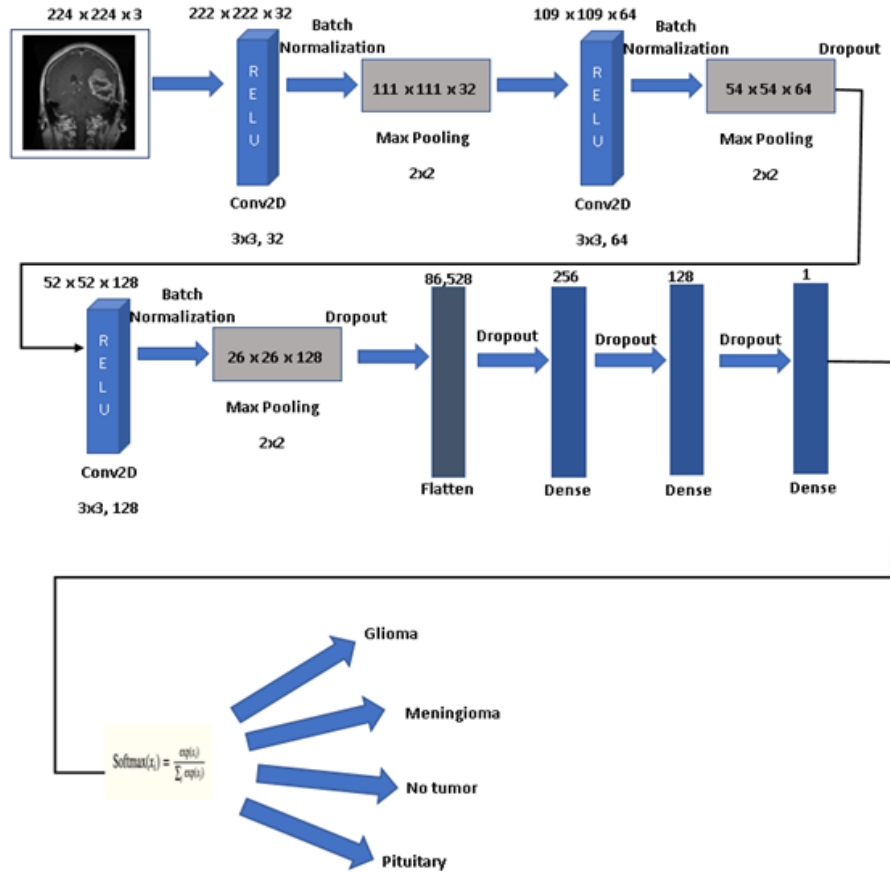


FIGURE 2. The detailed structure of the CNN model

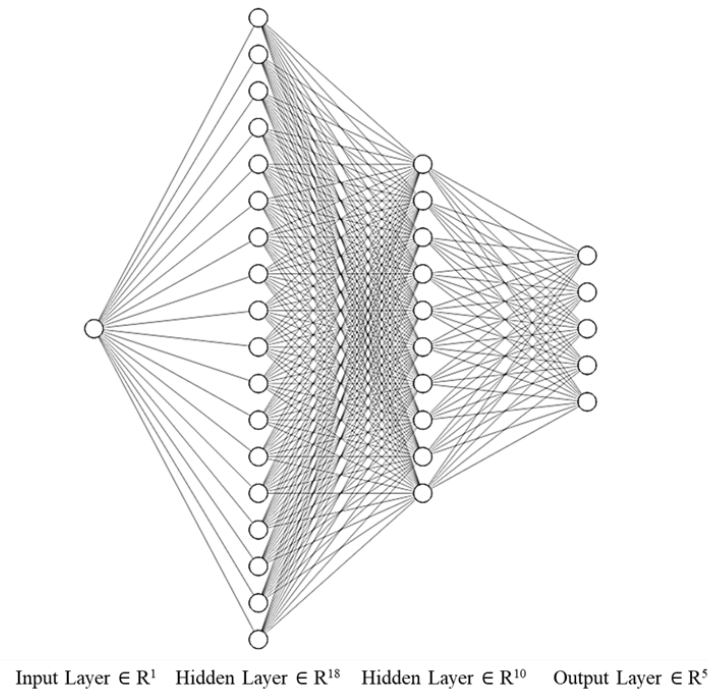


FIGURE 3. The proposed neural network structure

After optimizing the feature space, the KNN algorithm is used for final classification [27]. KNN training involves splitting batches into training and test sets, while extracting performance metrics across all epochs. This hybrid approach aims to improve

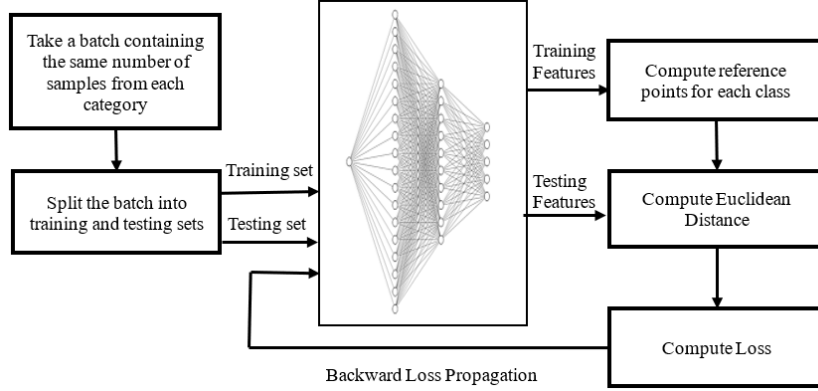


FIGURE 4. The training mechanism of the proposed artificial neural network

classification accuracy by leveraging deep feature extraction, dimensionality reduction, and efficient distance-based classification, contributing to more accurate and reliable brain tumor detection. Figure 5 shows the detailed structure of the proposed methodology. Table 1 shows the KNN parameters setting.

TABLE 1. The KNN parameters setting

Parameter	Description	Value
n_neighbors	Number of neighbors	n_neighbors = 3
weights	Weight function used in prediction	distance
algorithm	Algorithm used to compute the nearest neighbors	auto
p	Power parameter for the Minkowski metric	p = 2 (Euclidean distance)

**3.4. Evaluation Matrices.** A confusion matrix (CM) is a table used to evaluate the performance of a model, especially in supervised learning [28, 29]. The structure of the confusion matrix (CM) is presented in Figure 6.

Where TP (True Positive) occurs when the model accurately identifies a positive result, TN (True Negative) happens when the model correctly identifies a negative result, FP (False Positive) is associated with model mistakenly predicts a positive result and finally, FN (False Negative) occurs when the model incorrectly predicts a negative result.

Performance measurements are assessed by using the following metrics:

$$\text{Recall} = \frac{TP}{TP + FN} \tag{1}$$

where can be understood as quantifies of the ratio of true positives that the model accurately identifies [30]:

$$\text{Precision} = \frac{TP}{TP + FP} \tag{2}$$

which measures the ratio of correct positive predictions to the total number of positive predictions made [31].

$$\text{Accuracy} = \frac{TP + TN}{TP + TN + FP + FN} \tag{3}$$

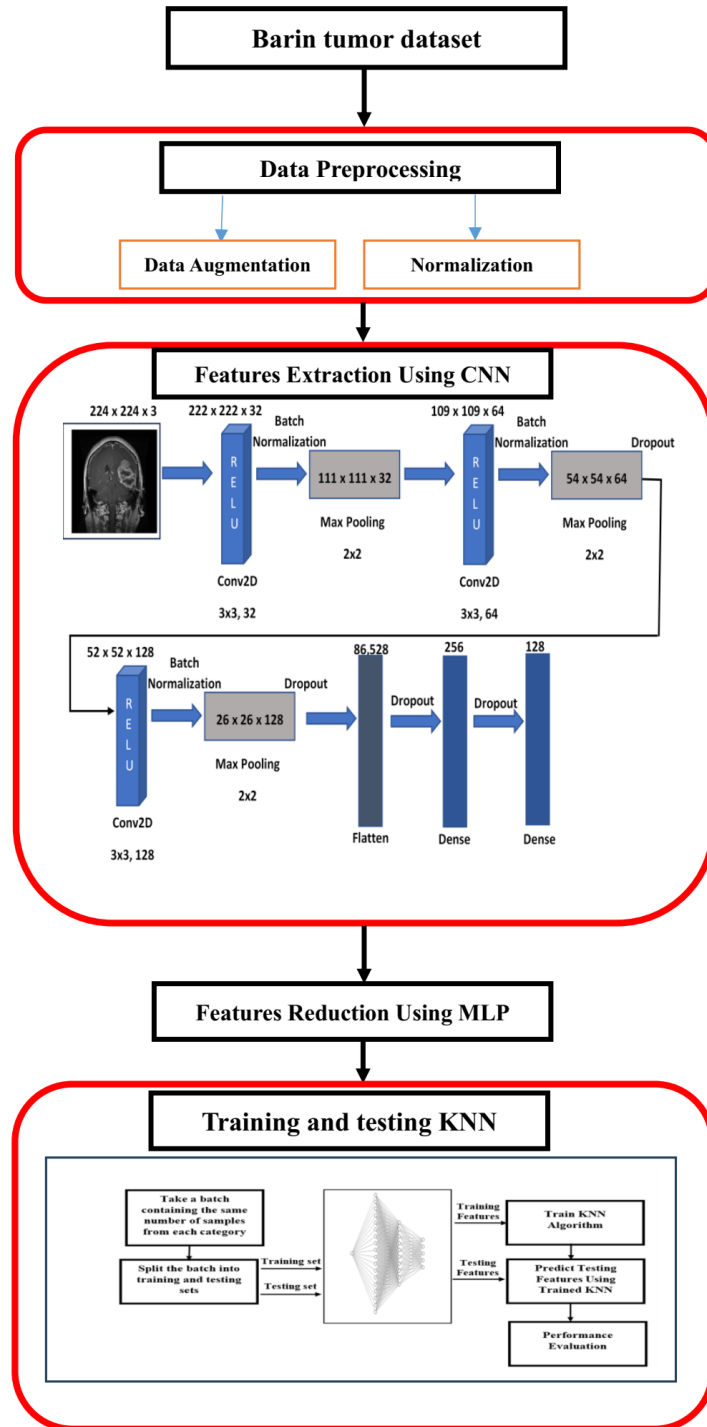


FIGURE 5. The detailed structure of the proposed methodology

which indicates the model’s overall performance by calculating the ratio of correct predictions—both positive and negative—compared to the total number of predictions made [32].

which presents a measurement that integrates precision and recall, offering a comprehensive assessment of a model’s overall effectiveness [33].

#### 4. Results and discussion.

		Actual Values	
		Positive (1)	Negative (0)
Predicted Values	Positive (1)	TP	FP
	Negative (0)	FN	TN

FIGURE 6. Confusion matrix architecture

4.1. **Motivation and contribution.** A learning curve is a graphical representation that displays the progression of a specific metric throughout the training phase of a model. The x-axis represents progress, while the y-axis reflects error or performance.

The representation is useful to check the changes that occur in the performance of the model during the learning phase, and enabling the detection of problems if they exist. One of the most common curves is the loss function curve, which shows the changes in the loss function (model errors) over time during the training phase. As the loss decreases, the performance of the model improves. The other learning curve is the accuracy curve, which measures the performance of the model during the training epochs, with increasing values of this curve indicating an improvement in the capabilities of the model. Figure 8 shows the accuracy and loss curves for both the training and validation runs of the custom CNNs shown in Figure 7.

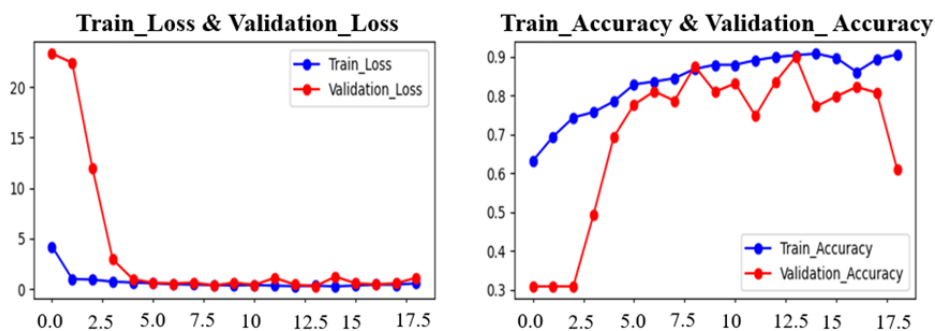


FIGURE 7. The accuracy and loss curves for both the training and validation processes for custom CNN

As shown in Figure 7, the performance of the custom CNN increases over the training epochs, with both the training and validation metrics trending upward. This indicates that the network’s performance improves on both the training (visible) and validation (unseen) data, suggesting successful convergence and better generalization, thereby mitigating the overfitting issue. In practice, the training process is deemed to have concluded at epoch 14, where the highest accuracy of 90% was achieved for both the training and validation data. We will now examine the results obtained from applying the custom CNN network to the test data, which consists of new, unseen data. Figure 9 presents the results of the confusion matrix generated by the CNN.

The main diagonal elements of the confusion matrix indicate the correct classifications performed by the custom CNN. The confusion matrix results show that the model accurately classified 237 samples from the glioma class, 247 samples from the meningioma

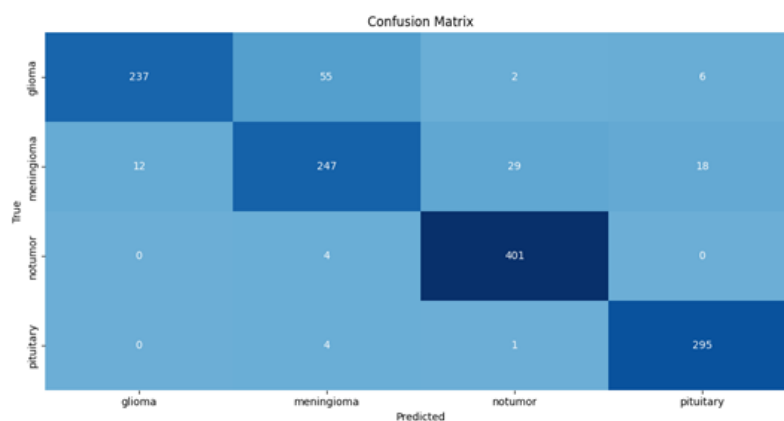


FIGURE 8. The results of the confusion matrix achieved by the custom CNN

class, 401 samples from the no-tumor class, and 295 samples from the pituitary class. Elements that are outliers of the main diagonal within the confusion matrix indicate to misclassifications. For instance, the element in the second row, first column (12) indicates that 12 samples of class Table 2 shows the custom CNN results based on Precision, Recall, and f1\_Score for each class.

TABLE 2. The custom CNN results based on Precision, Recall, and f1\_Score for each class

	Precision	Recall	F1_Score
Glioma	0.95	0.79	0.86
Meningioma	0.80	0.81	0.80
No-tumor	0.93	0.99	0.96
Pituitary	0.92	0.98	0.95

**Precision:** This metric measures the precision of the positive predictions made by the model, in other words, how many correct predictions the model made for a given class relative to the total number of predictions for that class. For example, the model achieved a high precision of 0.95 for glioma, meaning that when it predicted an image as a glioma, it was 95% correct.

**Recall:** This metric tells us the proportion of actual cases of a given tumor type that were correctly identified by the model. For example, the model achieved a recall of 0.79 for glioma, meaning that it correctly identified 79% of all glioma cases in the test dataset.

**F1-score:** This measure is the harmonic mean of precision and recall and provides a balanced measure of model performance. This measure can be used to determine the overall performance of the model and based on the results shown in Table 2, it can be said that the custom CNN performs well in classifying the No-tumor and Pituitary classes, achieving high F1\_Score values of 0.96 and 0.95, respectively. The CNN struggles in classifying the Glioma and Meningioma classes, achieving F1\_Scores of 0.86 and 0.80, respectively.

Based on the results shown in Table 2, we can conclude the overall performance of the custom CNN and calculate the overall accuracy of the system. Table 3 shows the overall performance of the custom CNN.

TABLE 3. The overall performance of the custom CNN

Precision	Recall	F1_Score	Accuracy
0.90	0.8925	0.8925	0.90

4.2. **Proposed Methodology Results.** Figure 9 shows the confusion matrix results for the proposed methodology.

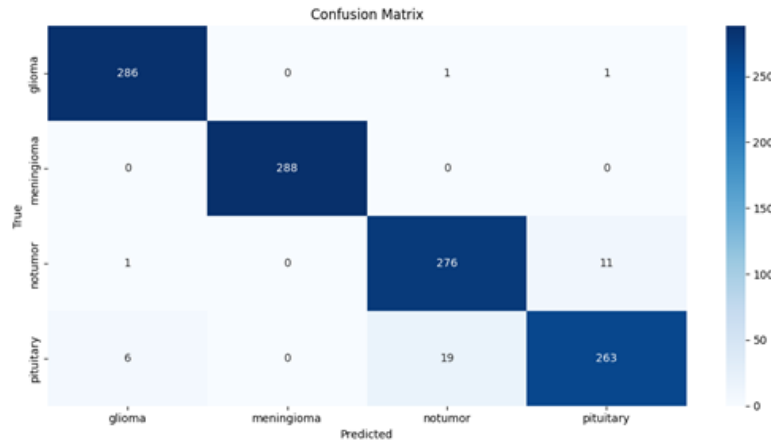


FIGURE 9. The confusion matrix results for the proposed methodology

We notice from the confusion matrix results that the majority of the classifications performed by the proposed model (main diagonal elements) are correct. The model failed in some classifications, for example, the proposed model classified 19 samples as no tumor while they are actually pituitary, and the model classified 11 samples as pituitary while they are actually no tumor, so there may be a similarity in the features of these two categories. The model succeeded in classifying all samples as meningioma. The model also succeeded in classifying 286 samples as glioma out of 289 samples, where it made mistakes in only two samples and classified one as no tumor and another as pituitary. Table 4 shows the proposed model results based on Precision, Recall, and f1\_Score for each class.

TABLE 4. The proposed model results based on Precision, Recall, and f1\_Score for each class

	Precision	Recall	F1_Score
Glioma	0.98	0.99	0.98
Meningioma	1.00	1.00	1.00
No-tumor	0.93	0.96	0.95
Pituitary	0.96	0.91	0.93

The results showed in Table 4 illustrate that the classification model effectively differentiates between tumor types and "no-tumor" cases, where the high precision across all classes minimizes false alarms, while the robust recall ensures comprehensive tumor detection. The balanced F1-scores demonstrate the model's consistency and reliability in accurately classifying MRI images into the respective categories.

For glioma, a precision of 0.98 indicates that of all the classifications that were classified as glioma, 98% were correct, indicating very few false positives. A recall of 0.99 indicates

that of all the actual glioma cases in the dataset, 99% were correctly classified, indicating very few false negatives. The F1\_Score of 0.98 reflects a strong balance between these metrics and confirms that the model is highly accurate in detecting gliomas.

For meningioma, a precision of 1.00 indicates that all classifications that were classified as meningioma were correct, indicating no false positives. A recall of 1.00 indicates that all meningioma cases in the dataset were correctly classified, indicating no false negatives. The F1\_Score of 1.00 also indicates flawless performance in detecting meningiomas.

For the No Tumor category, a precision of 0.93 indicates that of all predictions that were classified as “No Tumor”, 93% were correct, thus there were some false positives (tumor cases that were incorrectly classified as no tumor). The recall of 0.96 indicates that the model correctly classified 96% of the samples out of all the no-tumor samples in the dataset, thus there were a small number of false negatives. The F1\_Score of 0.95 indicates that the model performs well in classifying this category, but leaves room for slight improvement in distinguishing “No-Tumor” cases.

For the Pituitary category, a precision of 0.96 indicates that of all predictions that were classified as pituitary, 96% were correct, thus there were a small number of false positives. The recall value of 0.91 indicates that the model identified 91% of the actual bulimia cases in the dataset, indicating a slightly higher number of false negatives compared to the other categories. The F1\_Score value of 0.93 indicates a slight trade-off between precision and recall. Table 5 shows the overall performance of the proposed model.

TABLE 5. The overall performance of the proposed model

Precision	Recall	F1_Score	Accuracy
0.9675	0.965	0.9662	0.97

Comparing the overall performance of the proposed model shown in Table 5 with the overall performance of the custom CNN shown in Table 3, we note that:

- Using the proposed model, the precision value increased by about 6.75%, thus the proposed model significantly reduces false positives.
- Using the proposed model, the recall value increased by about 7.25%, thus the proposed model has a great ability to identify true positives with high efficiency.
- Using the proposed model, the F1\_Score value increased by about 7.37%.
- Using the proposed model, the overall accuracy increased by about 7%, thus the proposed model has high reliability in correctly classifying MRI images of brain tumors.

**5. Conclusions and future works.** Brain tumors are among the most sensitive tumors that must be detected in their very early stages, otherwise they will lead to irreparable problems in the body later. The main challenge in detecting brain tumors lies in the differences in tumor location, shape and size. Also, the tumor in its early stages is too small to be noticed by the human eye in MRI images, and thus doctors may misdiagnose the disease in its early stages. In this paper, we work to address the above-mentioned challenges by developing a hybrid model for automated brain tumor detection based on machine learning and deep learning techniques. In the proposed model, CNNs were used to extract fine features from MRI images, and then the extracted features were processed using MLP network to reduce the feature space. The K-nearest Neighbors (KNN) algorithm was then used for the final classification process. The proposed model achieved significant improvements over the custom CNN across all performance metrics used, achieving an accuracy of 97%, which is 7% higher than the CNN that achieved an accuracy of 90%, and

a recall of 96.5%, which is 7.25% higher than the CNN that achieved a recall of 89.25%, and a precision of 96.75, which is 6.75% higher than the CNN that achieved a precision of 90%. The results indicate that the combination of deep learning and traditional machine learning techniques enhances the model's ability to generalize and distinguish between different tumor types and non-tumor conditions. While the proposed model demonstrates significant improvements over the custom CNN, a direct comparison with other state-of-the-art models such as VGG-16, ResNet-50, and Inception V3 was not conducted in this study. Future work could involve benchmarking the proposed methodology against these deep learning architectures to further validate its effectiveness. Additionally, larger and more diverse datasets can be used to ensure the robustness and generalization ability of the model. Other feature reduction or classification algorithms, such as ensemble methods, can also be explored to further improve the model's performance.

## REFERENCES

- [1] J. Amin, M. Sharif, A. Haldorai, M. Yasmin, and R. S. Nayak, "Brain tumor detection and classification using machine learning: a comprehensive survey," *Complex & Intelligent Systems*, vol. 8, no. 4, pp. 3161–3183, 2022, doi: 10.1007/s40747-021-00563-y.
- [2] S. K. M. S. Islam, M. A. A. Nasim, I. Hossain, D. M. A. Ullah, D. K. D. Gupta, and M. M. H. Bhuiyan, "Introduction of Medical Imaging Modalities," in *Data Driven Approaches on Medical Imaging*, Cham: Springer, 2023, pp. 1–25.
- [3] A. Medetalibeyoglu, Y. S. Velichko, E. M. Hart, and U. Bagci, "Foundational artificial intelligence models and modern medical practice," *BJR—Artificial Intelligence*, vol. 2, no. 1, p. ubae018, 2025, doi: 10.1093/bjrai/ubae018.
- [4] M. Assaad and H. F. Husari, "Intelligent handwritten identification using novel hybrid convolutional neural networks," *Cihan University-Erbil Scientific Journal*, vol. 8, no. 2, pp. 99–103, 2024, doi: 10.24086/issn.2519-6979.
- [5] Y. Liu, H. Pu, and D. W. Sun, "Efficient extraction of deep image features using convolutional neural network (CNN) for applications in detecting and analysing complex food matrices," *Trends in Food Science and Technology*, vol. 113, pp. 193–204, 2021, doi: 10.1016/j.tifs.2021.04.042.
- [6] K. Zhao, J. Xiao, C. Li, Z. Xu, and M. Yue, "Fault diagnosis of rolling bearing using CNN and PCA fractal based feature extraction," *Measurement: Journal of the International Measurement Confederation*, vol. 223, p. 113754, 2023, doi: 10.1016/j.measurement.2023.113754.
- [7] M. Assaad, R. Boné, and H. Cardot, "A new boosting algorithm for improved time-series forecasting with recurrent neural networks," *Information Fusion*, vol. 9, no. 1, pp. 41–55, Jan. 2008, doi: 10.1016/j.inffus.2006.10.009.
- [8] S. U. Umar, T. A. Rashid, A. M. Ahmed, B. A. Hassan, and M. R. Baker, "Modified Bat Algorithm: a newly proposed approach for solving complex and real-world problems," *Soft Computing*, vol. 28, no. 13, pp. 7983–7998, Jul. 2024, doi: 10.1007/s00500-024-09761-5.
- [9] H. O. Ahmad and S. U. Umar, "An improved BAT algorithm for solving job scheduling problems in hotels and restaurants," *Informatika*, vol. 47, no. 5, pp. 153–158, 2023, doi: 10.31449/inf.v47i5.4673.
- [10] T. A. Rashid *et al.*, "An improved BAT algorithm for solving job scheduling problems in hotels and restaurants," in *Artificial Intelligence: Theory and Applications*, E. Pap, Ed. Cham: Springer International Publishing, 2021, pp. 155–171.
- [11] S. U. Umar and T. A. Rashid, "Critical analysis: bat algorithm-based investigation and application on several domains," *World Journal of Engineering*, vol. 18, no. 4, pp. 606–620, 2021, doi: 10.1108/WJE-10-2020-0495.
- [12] H. Khalid, "Deep learning algorithm for predicting various retail store sales using LSTM and ARIMA," *Dijlah Journal*, vol. 6, no. 4, pp. 348–362, 2023. [Online]. Available: <https://www.iraqoj.net/iasj/download/1440d5c45322515d>
- [13] H. Khalid, "Efficient image annotation and caption system using deep convolutional neural networks," *BIO Web of Conferences*, vol. 97, no. 3, p. 103, 2024, doi: 10.1051/bioconf/20249700103.
- [14] H. Khalid, "Modern techniques in detecting, identifying and classifying fruits according to the developed machine learning algorithm," *Journal of Applied Research and Technology*, vol. 22, no. 2, pp. 219–229, 2024, doi: 10.22201/icat.24486736e.2024.22.2.2269.

- [15] M. Assaad and R. Mahrousseh, “Improving some techniques for identifying people from ear prints,” *Tartous University Journal of Research and Scientific Studies—Series of Basic Sciences*, vol. 3, no. 2, 2019.
- [16] P. Ghosal, L. Nandanwar, S. Kanchan, A. Bhadra, J. Chakraborty, and D. Nandi, “Brain tumor classification using ResNet-101 based squeeze and excitation deep neural network,” in *2019 Second International Conference on Advanced Computational and Communication Paradigms (ICACCP)*, Gangtok, India, 2019: IEEE, pp. 1–6, doi: 10.1109/ICACCP.2019.8882973.
- [17] S. Krishnapriya and Y. Karuna, “Pre-trained deep learning models for brain MRI image classification,” *Frontiers in Human Neuroscience*, vol. 17, p. 1150120, 2023, doi: 10.3389/fnhum.2023.1150120.
- [18] N. Abiwinanda, M. Hanif, S. T. Hesaputra, A. Handayani, and T. R. Mengko, “Brain tumor classification using convolutional neural network,” in *World Congress on Medical Physics and Biomedical Engineering 2018*, Singapore, L. Lhotska, L. Sukupova, I. Lacković, and G. S. Ibbott, Eds. Singapore: Springer Nature, 2019, pp. 183–189, doi: 10.1007/978-981-10-9035-6\_33.
- [19] A. Pashaei, H. Sajedi, and N. Jazayeri, “Brain tumor classification via convolutional neural network and extreme learning machines,” in *2018 IEEE Int. Conf. Computing in Knowledge-Based Engineering (ICCKE)*, 2018: IEEE, pp. 314–319, doi: 10.1109/ICCKE.2018.8566571.
- [20] E. S. Biratu, F. Schwenker, T. G. Debelee, S. R. Kebede, W. G. Negera, and H. T. Molla, “Enhanced region growing for brain tumor MR image segmentation,” *Journal of Imaging*, vol. 7, no. 2, p. 22, 2021, doi: 10.3390/jimaging7020022.
- [21] M. Assaad and G. H. Shakah, “Optimizing health pattern recognition particle swarm optimization approach for enhanced neural network performance,” *Cihan University-Erbil Scientific Journal*, vol. 8, no. 2, pp. 76–83, 2024, doi: 10.24086/issn.2519-6979.
- [22] M. Nickparvar, “Brain Tumor MRI Dataset,” *Kaggle*, 2024. [Online]. Available: <https://www.kaggle.com/datasets/masoudnickparvar/brain-tumor-mri-dataset?select=Training>
- [23] A. Mumuni and F. Mumuni, “Data augmentation: a comprehensive survey of modern approaches,” *Array*, vol. 16, p. 100258, 2022, doi: 10.1016/j.array.2022.100258.
- [24] S. Azizi *et al.*, “Robust and data-efficient generalization of self-supervised machine learning for diagnostic imaging,” *Nature Biomedical Engineering*, vol. 7, no. 6, pp. 756–779, 2023, doi: 10.1038/s41551-023-01049-7.
- [25] P. Sane and R. Agrawal, “Pixel normalization from numeric data as input to neural networks: for machine learning and image processing,” in *2017 Int. Conf. Wireless Communications, Signal Processing and Networking (WiSPNET)*, Chennai, India, 2017: IEEE, pp. 2221–2225, doi: 10.1109/WiSPNET.2017.8300154.
- [26] F. Yang, H. Moayedi, and A. Mosavi, “Predicting the degree of dissolved oxygen using three types of multi-layer perceptron-based artificial neural networks,” *Sustainability (Switzerland)*, vol. 13, no. 17, p. 9898, 2021, doi: 10.3390/su13179898.
- [27] S. Uddin, I. Haque, H. Lu, M. A. Moni, and E. Gide, “Comparative performance analysis of K-nearest neighbour (KNN) algorithm and its different variants for disease prediction,” *Scientific Reports*, vol. 12, no. 1, p. 6256, 2022, doi: 10.1038/s41598-022-10358-x.
- [28] S. Haghighi, M. Jasemi, S. Hessabi, and A. Zolanvari, “PyCM: multiclass confusion matrix library in Python,” *Journal of Open Source Software*, vol. 3, no. 25, p. 729, 2018, doi: 10.21105/joss.00729.
- [29] I. Markoulidakis, I. Rallis, I. Georgoulas, G. Kopsiaftis, A. Doulamis, and N. Doulamis, “Multi-class confusion matrix reduction method and its application on Net Promoter Score classification problem,” *Technologies*, vol. 9, no. 4, pp. 412–419, 2021, doi: 10.3390/technologies9040081.
- [30] K. Roth, L. Pemula, J. Z. a, B. Schölkopf, T. Brox, and P. Gehler, “Towards total recall in industrial anomaly detection,” *arXiv preprint*, vol. arXiv:2106.08265, 2022, doi: 10.48550/arXiv.2106.08265.
- [31] S. J. MacEachern and N. D. Forkert, “Machine learning for precision medicine,” *Genome*, vol. 64, no. 4, pp. 416–425, Apr. 2021, doi: 10.1139/gen-2020-0131.
- [32] G. Fu *et al.*, “A deep-learning-based approach for fast and robust steel surface defects classification,” *Optics and Lasers in Engineering*, vol. 121, pp. 397–405, Oct. 2019, doi: 10.1016/j.optlaseng.2019.05.005.
- [33] D. Chicco and G. Jurman, “The advantages of the Matthews correlation coefficient (MCC) over F1 score and accuracy in binary classification evaluation,” *BMC Genomics*, vol. 21, no. 1, p. 1, 2020, doi: 10.1186/s12864-019-6413-7.